Monte Carlo Electron-Photon Interactions with Pair Formation

Chengchao Yuan
School of Astronomy & Space Science, Nanjing University
Supervisor: Prof. Peter Mészáros
Dept. of Astron. & Astrophysics, The Pennsylvania State University

1 Scientific Goals

1. Write a code in C++ to solve the kinetic equations of relativistic electrons in an isotropic photon field, including synchrotron, inverse Compton , $e^+ - e^-$ pair production and pair annihilation.

2. Calculate the interactions between extragalactic gamma-ray background (EGB) photons and the cosmic Microwave-Infrared background.

2 Radiation Processes from Relativistic Electrons

We consider an isotropic plasma containing relativistic electrons, positrons and photons, and the system is replenished by a time-independent magnetic field. All calculations are performed in the comoving frame, thus, the distributions of photons and particles can be assumed to be homogeneous and isotropic. From the conservation of energy we can write the equation

$$\frac{\mathrm{d}}{\mathrm{dt}}u_\gamma(t)\Phi(\epsilon,t) = \left[\frac{\partial}{\partial t}\nu(\epsilon,t)\right]_{\mathrm{sy+IC+pair}} \tag{1}$$

where $u_\gamma(t)$ is total energy density of photons at time t in the unit of erg cm^{-3} and the right-hand side $\frac{\partial}{\partial t}\nu(\epsilon,t)$ represents the total emissivity of synchrotron, IC and pair processes. Here, the instantaneous radiation spectrum is characterized by $\Phi(\epsilon,t)$ and $\epsilon = h\nu/m_e c^2$.

To solve the kinetic equation, we iterate the difference form

$$\Phi(\epsilon,t+\Delta t) = \Phi(\epsilon,t) + \frac{\Delta t}{u_\gamma(t)}\left[\frac{\partial}{\partial t}\nu(\epsilon,t) - \Phi(\epsilon,t)\frac{\mathrm{d}}{\mathrm{dt}}u_\gamma(t)\right], \tag{2}$$

$$\frac{\mathrm{d}}{\mathrm{dt}}u_\gamma(t) = \int_{\epsilon_{min}}^{\epsilon_{max}} \frac{\partial}{\partial t}\nu(\epsilon,t)\mathrm{d}\epsilon, \tag{3}$$

$$u_\gamma(t+\Delta t) = u_\gamma(t) + \Delta t\frac{\mathrm{d}}{\mathrm{dt}}u_\gamma(t). \tag{4}$$

As we can see from these equations, the most important task is to calculate the emissivity of synchrotron, IC, pair annihilation and the energy loss rate from pair creation.

2.1 Synchrotron

In the following calculations the electrons are assumed to be highly relativistic ($\gamma_{min}, \bar{\gamma} \gg 1$) and isotropic, moreover, the energy increase by synchrotron self-absorption is neglected. For the highly relativistic case ($\beta = v/c \approx 1$, $\gamma \gg 1$), the power per unit frequency emitted by each electron is

$$P(\omega,\gamma) = \frac{\sqrt{3}q^3 B\sin\theta_p}{2\pi m_e c^2}F(X) \tag{5}$$

where, θ_p is the angle between electron velocity direction and the magnetic field, $X = \omega/\omega_c$, $\omega_c = \frac{3}{2}\gamma^2 \frac{qB}{m_e c}\sin\theta_p$. $F(X)$ is given by

$$F(X) = X \int_X^\infty K_{5/3}(\eta) d\eta \tag{6}$$

where $K_{5/3}(\eta)$ is modified Bessel function. Utilizing the relationship $P(\omega,\gamma)d\omega = P(\epsilon,\gamma)d\epsilon$, we obtain the radiated power as a function of ϵ and γ

$$P(\epsilon,\gamma) = P(\omega,\gamma)\left|\frac{d\omega}{d\epsilon}\right| = \frac{\sqrt{3}q^2 B\sin\theta_p}{h} F\left(\frac{2m_e^2 c^3 \epsilon}{3\gamma^2 qB\sin\theta_p \hbar}\right). \tag{7}$$

The total power radiated per unit volume per unit ϵ by a normalized electron distribution $F_e(\gamma)$ is given by the integral of $F_e(\gamma)d\gamma$ times the single particle radiation formula over all γ

$$\left[\frac{\partial}{\partial t}\nu(\epsilon,t)\right]_{sy} = n_e \int_{\gamma_{min}}^{\gamma_{max}} P(\epsilon,\gamma) F_e(\gamma) d\gamma, \tag{8}$$

where n_e is the density of electrons. **General formulae are required to calculate the emissivity when this process is dominated by cyclosynchrotron** ($\gamma \approx> 1$) **or self-absorption plays a significant role.**

2.2 Inverse Compton scattering

The characteristic cooling time for IC is $t_c \approx q/\lambda c n_e \sigma_T \bar{\gamma}^2$ **where** q **is a dimensionless constant in order of unity and** $\lambda = u_\gamma/u_0$**. For typical GRB conditions, we have** $t_{acc,e} \ll t_c \ll \Delta/c$**, here** Δ **is the width of the emitting region in the comoving frame. Thus the cooling process occurs locally. According to Pilla & Loeb (1998), if** $\zeta_B \ll \zeta_e$**, the synchrotron cooling time is long and we must take multiple IC scattering into consideration, here the magnetic parameter** $\zeta_B = B^2/8\pi n_e m_p c^2(\bar{\gamma}_p - 1)$**, the electron parameter** $\zeta_e = \bar{\gamma}_0 m_e/(\bar{\gamma}_p - 1)m_p$ **and the average Lorentz factor of protons** $\bar{\gamma}_p \approx 3$**.** The the second term of equation(1)'s right-hand side from **multiple IC scattering** is

$$\left[\frac{\partial}{\partial t}\nu(\epsilon,t)\right]_{IC} = \frac{u_\gamma}{2T}\int_{-1}^{1} d\mu(1-\mu)\int_{\gamma_l}^{\gamma_{max}} d\gamma F_e(\gamma)\frac{\Phi(\epsilon,t)}{\langle\gamma^2\rangle_0}\zeta\frac{\sigma_{KN}}{\sigma_T} \tag{9}$$

where μ is the cosine of the scattering angle, $1/T = c n_e \sigma_T \langle\gamma^2\rangle_0$, $\gamma_l = \max(\gamma_{\min}, \epsilon)$, $\zeta = \gamma/(\gamma-\epsilon) = 1 + 2\gamma(1-\mu)\epsilon_1$, $\epsilon_1 = \epsilon/2\gamma(1-\mu)(\gamma-\epsilon)$ and $\sigma_{KN} = 3\sigma_T(\zeta^2 - 2\zeta/3 + 1)/4\zeta^3$ is the Klein-Nishina cross section. By integrating both sides of equation(9) over ϵ, we obtain $(du_\gamma/dt)_{IC}$. Here we use the relation $|d\epsilon/d\epsilon_1| = 2(1-\mu)\gamma^2/\zeta^2$ to convert the integral to be over ϵ_1. Finally we divide the integral by 2 to avoid the double accounting of the scattering and we get

$$\left(\frac{du_\gamma}{dt}\right)_{IC} = \frac{u_\gamma}{2T}\int_{-1}^{1} d\mu(1-\mu)^2\int_{\gamma_{min}}^{\gamma_{max}} d\gamma F_e(\gamma)\int_{\epsilon_{min}}^{\epsilon_{max}} d\epsilon_1 \Phi(\epsilon_1,t)\frac{\gamma^2}{\langle\gamma^2\rangle_0}\frac{1}{\zeta}\frac{\sigma_{KN}}{\sigma_T}. \tag{10}$$

2.3 Pair creation

The production rate of $e^+ - e^-$ with Lorentz factor in the range γ to $\gamma + d\gamma$ by an isotropic photon field with photon density $n_{ph}(\epsilon,t) = u_\gamma(t)\Phi(\epsilon,t)/(\epsilon m_e c^2)$ is

$$\begin{aligned}\frac{\partial}{\partial t}n_{eP}(\gamma,t) = \frac{3}{4}\sigma_T c\int_0^\infty d\epsilon_1 \frac{n_{ph}(\epsilon_1,t)}{\epsilon_1^2}\int_{max(1/\epsilon_1,\gamma+1-\epsilon_1)}^\infty d\epsilon_2\frac{n_{ph}(\epsilon_2,t)}{\epsilon_2^2} \\ \times\left(\frac{\sqrt{E^2-4\epsilon_{cm}^2}}{4} + H_+ + H_-\right)_{\epsilon_{cm}^L}^{\epsilon_{cm}^U};\end{aligned} \tag{11}$$

$\epsilon_{1,2}$ are the scattering photons energies in the unit of $m_e c^2$, $E = \epsilon_1 + \epsilon_2$, and ϵ_{cm} is the photon energy in the center-of-momentum frame, given by $\epsilon_{cm} = \sqrt{2\epsilon_1\epsilon_2}$. The functions $H_\pm$ are calculated using

$$c_\pm = (\epsilon_{1,2} - \gamma)^2 - 1, \tag{12}$$

$$d_\pm = \epsilon_{1,2}^2 + \epsilon_1\epsilon_2 \pm \gamma(\epsilon_2 - \epsilon_1). \tag{13}$$

For $c_\pm \neq 0$, $H_\pm$ are given by

$$\begin{aligned} H_\pm = &- \frac{\epsilon_{cm}}{8\sqrt{\epsilon_1\epsilon_2 + c_\pm\epsilon_{cm}^2}}\left(\frac{d_\pm}{\epsilon_1\epsilon_2} + \frac{2}{c_{pm}}\right) \\ &+ \frac{1}{4}\left(2 - \frac{\epsilon_1\epsilon_2 - 1}{c_\pm}\right) I_\pm \\ &+ \frac{\sqrt{\epsilon_1\epsilon_2 + c_\pm\epsilon_{cm}^2}}{4}\left(\frac{\epsilon_{cm}}{c_\pm} + \frac{1}{\epsilon_{cm}\epsilon_1\epsilon_2}\right), \end{aligned} \tag{14}$$

where

$$I_\pm = \begin{cases} \frac{1}{\sqrt{c_\pm}}\ln\left(\epsilon_{cm}\sqrt{c_\pm} + \sqrt{\epsilon_1\epsilon_2 + c_\pm\epsilon_{cm}^2}\right), c_\pm > 0; \\ \frac{1}{\sqrt{-c_\pm}}\arcsin\left(\epsilon_{cm}\sqrt{-\frac{c_\pm}{\epsilon_1\epsilon_2}}\right), c_\pm < 0. \end{cases} \tag{15}$$

For $c_\pm = 0$,

$$H_\pm = \left(\frac{\epsilon_{cm}^3}{12} - \frac{\epsilon_{cm}d_\pm}{8}\right)\frac{1}{(\epsilon_1\epsilon_2)^{3/2}} + \left(\frac{\epsilon_{cm^3}}{6} + \frac{\epsilon_{cm}}{2} + \frac{1}{4\epsilon_{cm}}\right)\frac{1}{\sqrt{\epsilon_1\epsilon_2}} \tag{16}$$

The upper and lower integration limits in equation (11) are given by

$$\epsilon_{cm}^U = \min(\sqrt{\epsilon_1\epsilon_2}, \epsilon_{cm}^a), \epsilon_{cm}^L = \max(1, \epsilon_{cm}^b), \tag{17}$$

where

$$(\epsilon_{cm}^{a,b})^2 = \frac{1}{2}\{\gamma(E-\gamma) + 1 \pm \sqrt{[\gamma(E-\gamma)+1]^2 - E^2}\}. \tag{18}$$

The total loss rate of photons in the energy interval ϵ_1 to $\epsilon_1 + d\epsilon_1$ by pair creation is

$$R_P(\epsilon_1, t) = -n_{ph}(\epsilon_1, t)\frac{c}{2}\int d(\cos\theta)(1-\cos\theta)\int_{2/\epsilon_1(1-\cos\theta)}^{\infty} d\epsilon_2 n_{ph}(\epsilon_2, t)\sigma(\epsilon_1, \epsilon_2, \theta) \tag{19}$$

here, the cross section is given by

$$\sigma(\epsilon_1, \epsilon_2, \theta) = \frac{3}{16}\sigma_T(1-\beta'^2)\left[2\beta'(\beta'^2 - 2) + (3 - \beta'^3)\ln\left(\frac{1+\beta'}{1-\beta'}\right)\right] \tag{20}$$

and

$$\beta' = \left[1 - \frac{2}{\epsilon_1\epsilon_2(1-\cos\theta)}\right]^{1/2}. \tag{21}$$

In this code, the loss rate of radiation energy density is obtained using equation(19)

$$\left[\frac{\partial}{\partial t}\nu(\epsilon_1, t)\right]_{\text{pair\_creation}} = \epsilon_1 m_e c^2 R_{ph}(\epsilon_1, t). \tag{22}$$

The spectra of emergent electrons and positrons can be calculated utilizing equation(11), **here we follow Péer & Waxman (2005) that the spectrum of emerging pairs is determined by the photon energies: (1) For $1.01 \leq \epsilon_1\epsilon_2 \leq 10^4$, the exact spectrum can be obtained by solving equation(11). (2) For $\epsilon_1\epsilon_2 \leq 1.01$, a monochromatic spectrum of the created particles is assumed, with energy $(\epsilon_1 + \epsilon_2)/2$. (3) If $\epsilon_1\epsilon_2 \geq 10^4$, the energies of created particles are taken to be $\gamma_1' = \max(\epsilon_1, \epsilon_2)$ and $\gamma_2' = \min(\epsilon_1, \epsilon_2) + 1/[2\min(\epsilon_1, \epsilon_2)]$ respectively.**

2.4 Pair annihilation

The total loss rate of electrons with Lorentz factor from γ_1 to $\gamma_1 + d\gamma_1$ due to pair annihilation is given by

$$\frac{\partial n_{e^- Anni}(\gamma_1,t)}{\partial t} = -n_{e^-}(\gamma_1,t)\frac{c}{2\gamma_1}\int d(\cos\theta)\int d\gamma_2 n_{e^+}(\gamma_2,t)\beta_2^{'}\frac{dn^{'}}{dn}\sigma_{\rm anni}(\gamma_2^{'}), \tag{23}$$

where $\gamma_2^{'} = \gamma_1\gamma_2(1+\beta_1\beta_2\cos\theta)$ is the Lorentz factor of positron in the electron-rest frame, $\beta^{'}$ is the corresponding velocity in this frame and $dn^{'}/dn = \gamma_1(1+\beta_1\beta_2\cos\theta)$. The cross section $\sigma_{\rm anni}$ for the annihilation between a positron with Lorentz factor γ_1 and a rest electron is

$$\sigma_{\rm anni}(\gamma) = \frac{3}{8}\frac{\sigma_T}{\gamma+1}\left[\frac{\gamma^2+4\gamma+1}{\gamma^2-1}\ln\left(\gamma+\sqrt{\gamma^2-1}\right) - \frac{\gamma+2}{\sqrt{\gamma^2-1}}\right] \tag{24}$$

The loss rate of positrons is calculated in the similar way. **As shown in Svensson (1982), the photon spectrum is narrowly concentrated around the energies of annihilated particles, $(\gamma_{1,2}m_ec^2)$. To obtain the increase rate spectra of photons, we assume that the emergent photons with dimensionless energies $\epsilon_{1,2}$ are generated from pairs having the Lorentz factors $\gamma_{1,2} \approx \epsilon_{1,2}$, which means** $e^+(\gamma_1) + e^-(\gamma_2) \rightarrow photon_1(\epsilon_1 = \gamma_1) + photon_2(\epsilon_2 = \gamma_2)$. Thus we have

$$\left[\frac{\partial}{\partial t}\nu(\epsilon=\gamma,t)\right]_{\rm pair\_anni} = -\epsilon m_ec^2\frac{dn_{eA}(\gamma,t)}{dt} = -\epsilon m_ec^2\left[\frac{\partial n_{e^- Anni}(\gamma,t)}{\partial t} + \frac{\partial n_{e^+ Anni}(\gamma,t)}{\partial t}\right]. \tag{25}$$

So far, we have found all compositions of the total changing rate of radiation energy density and the right-hand side term of equation(1) can be calculated

$$\left[\frac{\partial}{\partial t}\nu(\epsilon,t)\right] = \sum_i\left[\frac{\partial}{\partial t}\nu(\epsilon,t)\right]_i, \tag{26}$$

here, the summation of i is carried out over the elements of aggregation S ={sy, IC, pair creation, pair annihilation}. In addition, if pair processes are included in the calculation, the electron/positron spectrum will evolve due to pair creation and pair annihilation in the way

$$n_{e^-,e^+}(t+\Delta t,\gamma) = n_{e^-,e^+}(t,\gamma) + \left[\frac{\partial}{\partial t}n_{eP}(\gamma,t) + \frac{\partial n_{e^-,e^+ Anni}(\gamma,t)}{\partial t}\right]\Delta t. \tag{27}$$

3 Numerical Methods

To calculate the single and multiple integrations in the left-hand side of equation(1) numerically, adaptive Simpson integral and adaptive Monte Carlo method are employed respectively. Details about adaptive Simpson integration can be found in the book *Numerical Recipes* and a brief introduction to adaptive Monte Carlo method is presented below.

The concrete procedures can be found in Pilla et al (1997). Before Pilla, a algorithm given by Lepage (1978) is widely used in particle physics and the code implementing this method, known as VEGAS, can be found in Press et al (1992). However, Pilla et al (1978) argues that there are some shortcomings in VEGAS, such as weak convergence and numerical instability in high energy tail. Because all of these, we use the method given by Pilla et al to solve multidimensional integrations. Here, we consider a one-dimensional integration $I = \int_0^1 f(x)dx$ without losing the generality and any characteristics of this method. At first, we need to discretize the domain of integration as $0 = x_0 < x_1 < x_2 < ..... < x_N = 1$ and $\Delta x_i = x_i - x_{i-1}$ for $i = 1, 2, ..., N$, where N is an integer great than 1. We use the following $p(x)$ as the normalized probability distribution,

$$p(x) = \frac{1}{N\Delta x_i},\ \text{if } x \in [x_{i-1}, x_i) \tag{28}$$

in order that $\int_{x_{i-1}}^{x_i} p(x)dx = 1/N$ for all i. Here, the bin sizes Δx_i need not to be equal but all bins have the same probability weight. Now the approximated result is $I \approx \sum_{k=1}^{M} f(\zeta_k)/Mp(\zeta_k)$, where ζ_k are uniformly distributed random numbers in the interval $[0, 1)$. In general, the integer M is much greater than N. Let

$$u_i = \frac{N}{M} \sum_{k=1}^{M} c_i(k) \left| f(\zeta_k) \right|, \tag{29}$$

where $c_i(k) = 1$, if $x_{i-1} < \zeta_k < x_i$ and $c_i(k) = 0$ otherwise. Obviously, $\sum_{i=1}^{N} u_i \Delta x_i = I$. Therefore, $w_i = u_i \Delta x_i / I$ is the importance weight of the i^{th} bin. Since different bins contribute different amounts of the integral, the idea now is to find a new discretization scheme $\{x_1, x_x, ..., x_N\}$ so that all bins have the same importance weight $1/N$. Let l be an integer such that

$$\sum_{m=1}^{l} w_m \leq i w_0 < \sum_{m=1}^{l+1} w_m. \tag{30}$$

The new boundary location of the i^{th} bin is given by

$$x_{i,\mathrm{new}} = x_{l,\mathrm{old}} + \frac{1}{w_0} \left(i w_0 - \sum_{m=1}^{l} w_m \right) (x_{l+1,\mathrm{old}} - x_{l,\mathrm{old}}) \tag{31}$$

However, in practice we must damp the convergence so that the contribution from the low importance bins is not overly suppressed. As in the method by Lepage, we will damp the convergence by using the modified importance weights given by

$$w_i^{'} = \left[\frac{1 - w_i}{\ln(1/w_i)} \right]^{\alpha} \tag{32}$$

which gives $w_0^{'} = \sum_{i=1}^{N} w_i^{'}/N$. We now replace w_0 and w_i with $w_0^{'}$ and $w_i^{'}$ and repeat this process iteratively until $\sum_{i=1}^{N} |x_{i,\mathrm{old}} - x_{i,\mathrm{new}}| \,/\, \sum_{i=1}^{N} |x_{i,\mathrm{old}} + x_{i,\mathrm{new}}| < \theta$ (here $\theta = 10^{-3}$), then we can obtain the desired result for I. In all our calculations, we follow Pilla et al to take $N = 70$, $\alpha = 1.3$ and $M = 20000$. It's easy to extend the scheme to multidimensional integrations.

Interpolation and functional approximation are used in the code to calculate the intensity of a discrete spectrum at an arbitrary energy and to obtain the modified Bessel function $K_{5/3}(x)$, respectively. For more details, please refer to *Numerical Recipes*.

4 Specific Astrophysical Calculations

4.1 Power law electrons

In this case, we use the same initial parameters and electron distributions as (Pilla & Loeb, 1998) to test the code: the magnetic field $B = 4.9 \times 10^4$ Gauss ($\zeta_B = 0.1$), electron density $n_e = 3.1 \times 10^{12}$ cm^{-3}, escape time of radiation $t_c = \Delta/c = 1.2s$, where Δ is the width of emitting region, and the minimum Lorentz factor $\gamma_{min,0} = 1656.46$ ($\zeta_e = 0.3$). The fraction of electrons per unit interval $d\gamma$ is $F_e(\gamma, t) = (p-1)\gamma_{min}(t)^{p-1}\gamma^{-p}$, where $\gamma_{min}(t) = \frac{p-2}{p-1}\bar{\gamma}(t)$. We assume that in the cooling process of electrons, the power law maintains a constant index $p = 3.5$ and with the increase of radiation energy density, the $\bar{\gamma}(t)$ is given by

$$u_0 = u_\gamma(t) + u_e(t) = u_\gamma(t) + n_e \bar{\gamma}(t) m_e c^2 \tag{33}$$

where $u_0 = n_e \bar{\gamma}_0 m_e c^2$ is the initial kinetic energy density of electrons.

We assume that the radiation energy density is initially small and, hence, the electrons start losing their energy via synchrotron emission. As the energy density of the emitted radiation builds

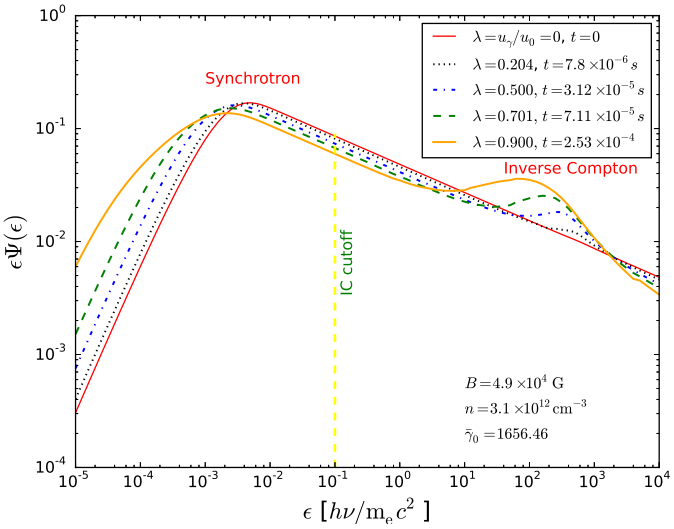

Figure 1: The evolution of spectrum in the early phase. In this phase λ increases to unity.

up, cooling via IC scattering becomes important as well. In this calculation, the pair creation comes into play after the electrons cool and decouple ($\lambda = u_\gamma/u_0 \approxeq 1$). Moreover, the pairs are relativistic when they are created; eventually, they transfer almost all their energy back to the radiation field via IC scattering and synchrotron which means the pairs are created but they do not annihilate.

Figure 1 illustrates the evolution of spectrum in the early phase when the process is dominated by IC and synchrotron. From this figure we find that with the spectrum evolving, the peak of synchrotron shifts to low energies and another peak develops due to IC scattering. When almost the kinetic energy is transferred to radiation, pair creation is activated and will dominate the subsequent evolution. Figure 2 shows the spectra of pair creation rate $\frac{\partial}{\partial t} n_{eP}(\gamma, t)$ (left) and radiation absorption rate $\epsilon m_e c^2 R_P(\epsilon_1, t)$ (right) immediately after pair creation is activated. From the left figure, the electrons creating rate increases rapidly at $\gamma > \approx 1$ and then decreases in a power-law function. Since the pair creation occurs when a high-energy photon interacts with a low-energy photon, there should be two absorption peaks and this is consistent with the right figure. The consequent evolution of the radiation spectrum can be found in figure 3. The high-energy photons exhaust rapidly due to pair creation and the increase of low-energy photons is not very conspicuous.

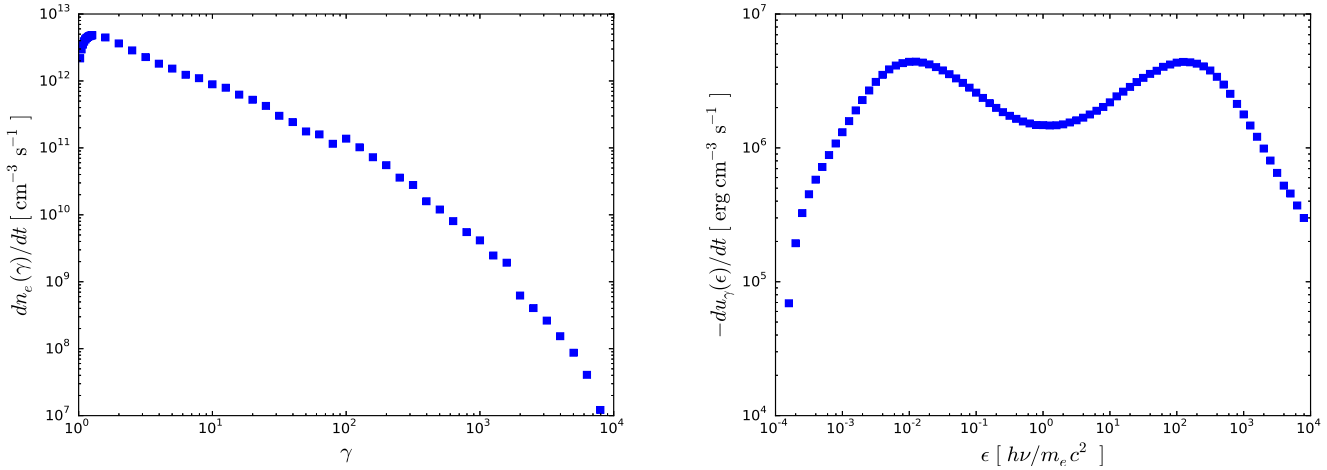

Figure 2: Spectra of pair creation rate (left) and photon energy density loss rate (right).

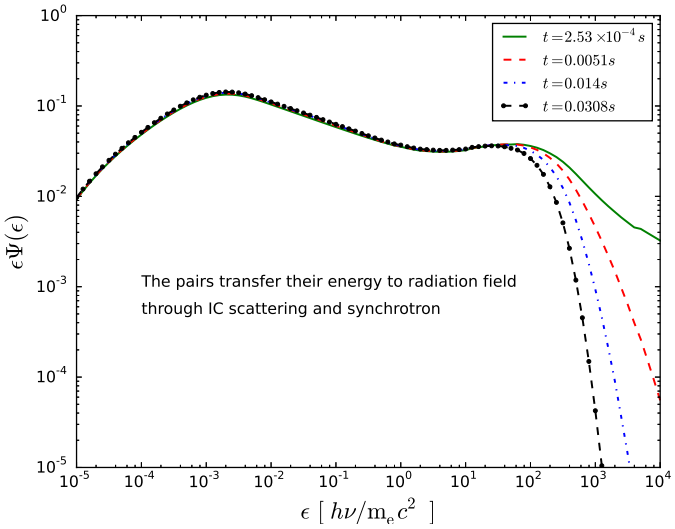

Figure 3: Subsequent evolution caused by pair creation

4.2 Thermal electrons

In this situation, the kinetic energy of electrons comes from thermal motion and the fraction of electrons per unit interval $d\gamma$ is described by the Maxwell-Boltzmann function

$$F_e(\gamma, t) = \frac{\alpha}{K_2(\alpha)}\beta\gamma^2 \exp(-\alpha\gamma), \tag{34}$$

where $\alpha = m_e c^2/kT(t)$, the velocity $\beta = (\gamma^2 - 1)^{1/2}/\gamma$ and k is the Boltzmann constant. The temperature of electron gas evolves with time in the way

$$u_0 = u_\gamma(t) + u_e = u_\gamma(t) + n_e kT(t) \tag{35}$$

Same initial quantities are used in this calculation except the initial temperature $T_0 = \bar{\gamma}_0 m_e c^2/k$. In the early phase, the evolution of spectrum is shown in figure 4. Similar conclusions can be obtained as in subsection 4.1 and the strong cut-off at high energy at $t = 0$ is caused by the exponential decrease of $F_e(\gamma, t)$.

4.3 Interactions between EGB and Microwave-Infrared background

High-energy γ-ray photons will interact with a low-energy photon backgrounds including Cosmic Microwave Background (CMB) and Extragalactic Background Light (EBL). As a result, e^+e^- pairs will be created and they will annihilate back to radiation field until the equilibrium state is realized. The EBL photons, concentrated in the energy range 10^{-3} to 10 eV, are believed to be the main cause of γ-ray cut-off at TeV. Figure 5 shows the measurements of EGB spectrum (Ackermann et al, 2014). Here, we calculate the interactions between EGB photons and CMB+EBL photons and try to interpret the IGRB cut-off at 10^5MeV.

Noting that temperature $T \propto (1 + z)$ and radiation density $\rho_\gamma \propto (1 + z)^4$, the CMB photon density per unit energy interval $d\epsilon$ at redshift $z \geq 0$ is given by

$$\left[\frac{dN}{d\epsilon dV}(\epsilon, z)\right]_{CMB} = (1+z)^4 \frac{8\pi}{\lambda_c^3} \frac{\epsilon^2}{\exp[\epsilon/\Theta(z)] - 1} \tag{36}$$

where $\lambda_c = h/m_e c \approx 2.42 \times 10^{-10}$cm is the Compton wavelength, $\Theta = (1 + z)kT_0/m_e c^2$ is the dimensionless effective temperature, and $T_0 = 2.73$ K. We use the "Model C" given by Finke et al

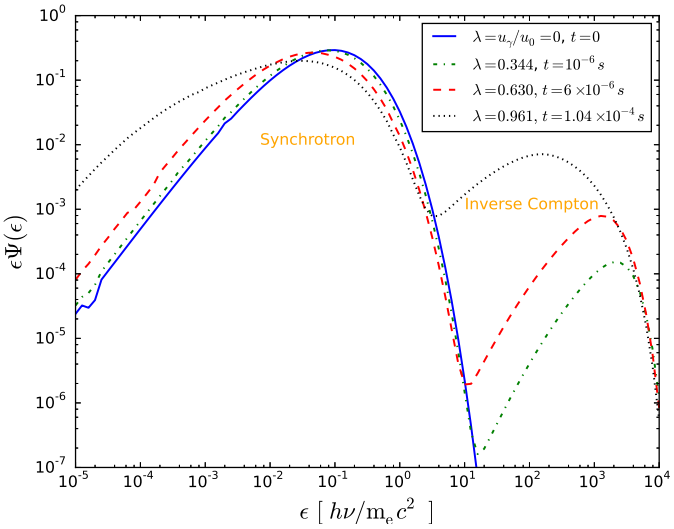

Figure 4: Early evolution of spectrum from thermal electrons

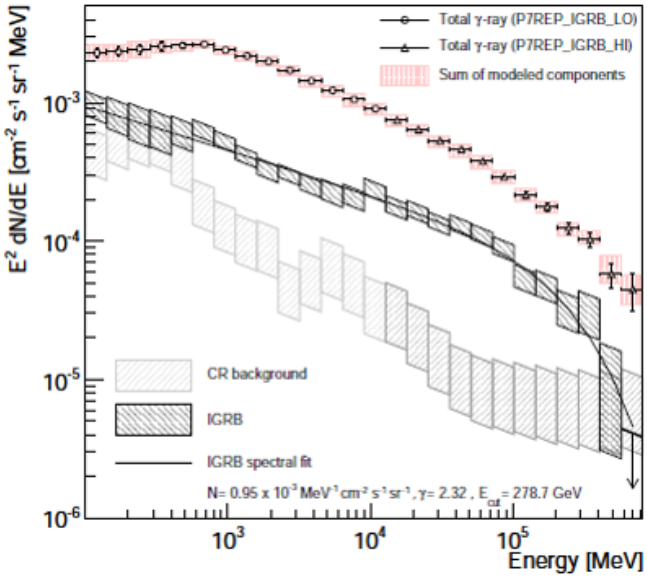

Figure 5: *Fermi* measurements of the extragalactic diffuse γ-ray background (Ackermann et al, 2014).

(2010) to obtain the energy density spectra of EBL at arbitrary redshifts (Figure 6). In our code, the spectrum evolves with respect to time, however, for a single $\gamma-$ray source located at redshift z, we must convert the integration of time to redshift. Assuming a ΛCDM universe with $\Omega_m = 0.3$ and $H_0 = 71$ km s^{-1} Mpc^{-1}, the relation between proper time and redshift is

$$\frac{dt}{dz} = -\frac{1}{H_0(1+z)\sqrt{\Omega_m + (1-\Omega_m)(1+z)^3}}. \tag{37}$$

Integrate equation(37) from z to 0, we get the time as a function of redshift, as shown in figure 7.

At first, we use a power law to fit the EGB spectra section from 10^2 GeV to 10^5 GeV and extend the fitting to higher energy ($E > 10^5$ GeV). Figure 8 (left) illustrates the input EGB spectrum and the local background spectra. The right figure shows the evolution of spectrum due to the interactions between $\gamma-$ray photons and background photons. If the background is CMB, we

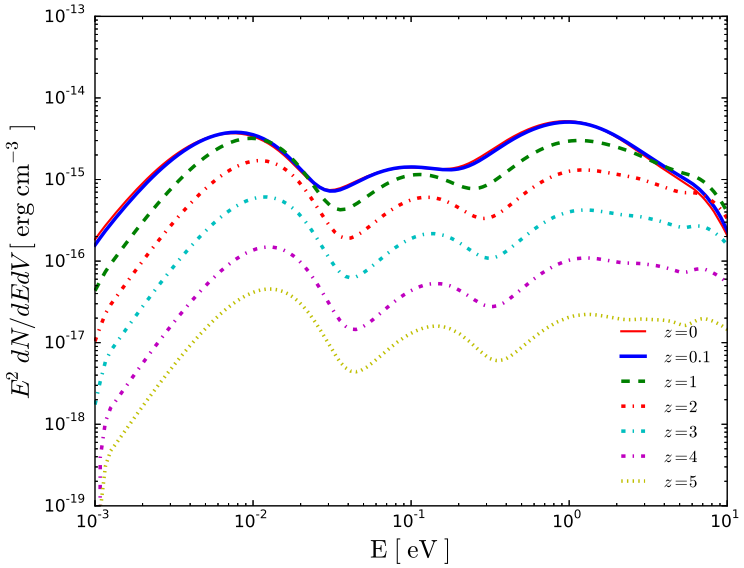

Figure 6: Model C for EBL spectra at different redshifts

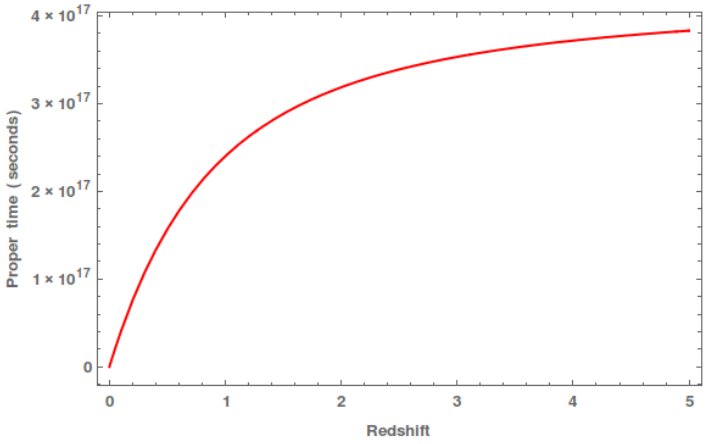

Figure 7: Relationship between redshift and proper time in the ΛCDM universe with $\Omega_m = 0.3$ and $H_0 = 71$ km s^{-1} Mpc^{-1}

find that the time scale required to obtain the equilibrium state is 10^{13} seconds which corresponds to the redshift $z \approx 10^{-4}$, so we neglect the redshift evolution of CMB spectra in this case. And we find a TeV cut-off due to CMB background. After including the component of EBL background, the results (dashed lines) are in agreement with the observed data.

Neutrinos and high-energy $\gamma-$rays are generated simultaneously when high-energy cosmic rays undergoes the *pp* interactions with ambient medium. Because of this, the relation of neutrino flux and $\gamma-$ray flux is (here, $\Gamma = 2$)

$$\epsilon_\gamma^2 \Phi_{\epsilon_\gamma} = 2^{\Gamma-1} \epsilon_\nu^2 \Phi_{\epsilon_\nu}|_{\epsilon_\nu = 0.5\epsilon_\gamma}. \tag{38}$$

In this calculation, we assume the EBL is produced by a single GRB and the neutrino flux can be found in Senno et al (2015). The input spectrum and the background are shown in Figure 9 (left). The right figure illustrates the evolution of neutrino-related $\gamma-$ray spectrum.

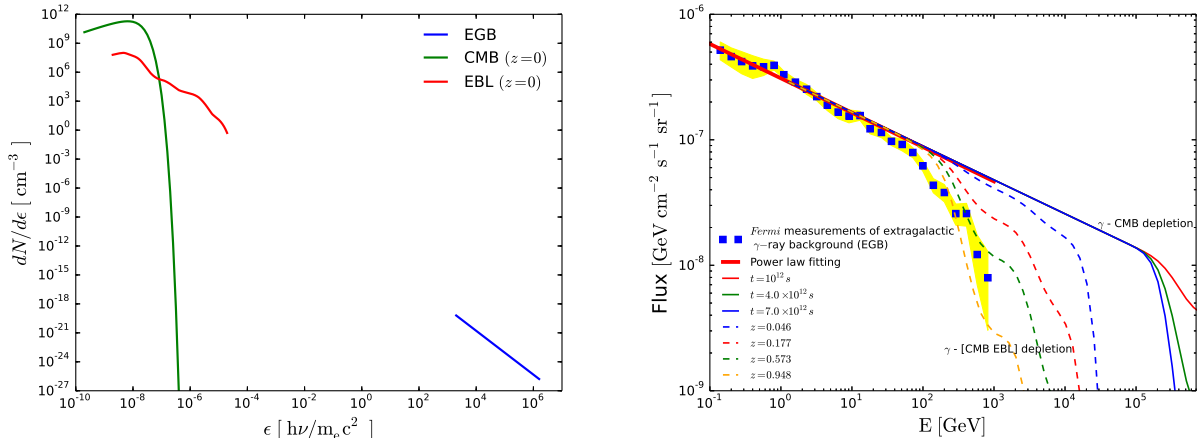

Figure 8: (Left) — The input EGB spectrum and the local background spectra; (Right) — The evolution of power-law EGB spectrum: solid lines represent the case that background is only CMB and if both CMB and EBL are included, we get the dashed lines.

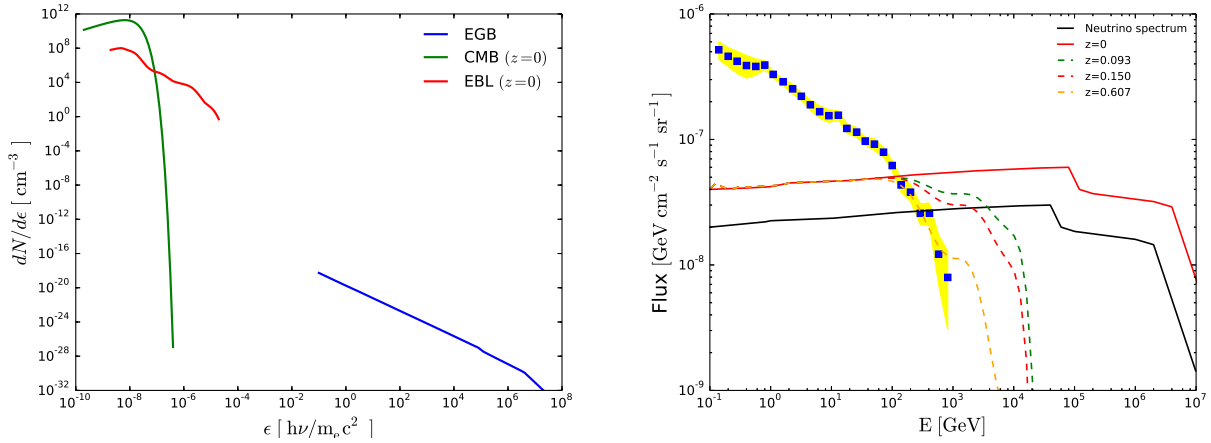

Figure 9: (Left)— The input EGB spectrum and the local background spectra; (Right)— Diffuse flux per flavor of neutrinos (solid black); Neutrino-related $\gamma-$ray spectrum under the single-source assumption (solid red); observed $\gamma-$ray spectra at different redshifts (dashed)

5 Discussions and Further Applications

1. This code is written in C++. To include the components of synchrotron, IC, pair production or pair annihilation in the calculation, just include the header files to the source file and invoke the corresponding function.

2. Since this code is used to solve the kinetic equations in the comoving frame, Lorentz transformation is required when calculate the spectrum evolution in a moving frame, such as GRB jet.

Two possible science projects to which one could apply this are as follows (This part is from Prof. Peter Mészáros):

1) Apply to photospheric gamma-ray bursts. Assume the photospheric radius is baryonic-dominated (i.e. not magnetic-dominated, see Veres et al, 2013, ApJ, 764:94, and Meszaros, P. and Rees, M.J., 2000, ApJ, 530, 292). Then consider a range of $L_{kin,iso}$ and Γ (isotropic equivalent kinetic luminosities and final Lorentz factors), say $L_{k,i} = [10^{51} - 10^{55}]$, Γ=[100-1000]. Assume that the comoving-frame photospheric spectrum is of an approximate Band-type, such that the peak tem-

perature is similar to the Planck temperature for that L_k, but various internal processes rearrange the low energy photon number slope to be -1 and the high energy slope to be -2 (to conserve energy you may need to lower the normalization so that total escaping energy does not exceed the blackbody limit). The comoving highest photon energy of the high energy slope could be 0.5 MeV (comptonization, see Veres et al) or it could be due to pion decay effects in the comoving frame (see Beloborodov, 2010, MNRAS 407:1033). Then with this comoving-frame spectrum, assume that photons are emitted isotropically from the baryonic photospheric radius (but in the outward hemisphere direction). You will also have to assume a jet opening angle, or width of emission region at the radius of the photosphere, say corresponding to 5 degrees). Then check

(a) whether pair formation extends the photosphere to radii further out than the originally assumed one (which was based on baryonic electrons only). If yes, then you will have to iterate the photospheric radius, readjusting the peak temperature to be that corresponding to that radius, and find the final photosphere radius.

(b) check at what energy occurs E_{cut}, the gamma-gamma cutoff in the high energy slope.

(c) convert this to an observer-frame energy and spectra, and check whether one obtains a correlation between L_k, Γ and E_{cut}.

2) Another possible application would be to the hypernova/starburst problem, where, as in the Senno et al (and other papers as well) the observed diffuse neutrino spectrum is expected to be 1/2 of the resulting diffuse gamma ray spectrum which is input into the IGM- but the EBL and CMB then reprocess it to give a final observed diffuse gamma spectrum which should not exceed the Fermi observed spectrum. One can use the redshift-dependent evolution of the starburst and starforming galaxies, and the redshift-dependence of the EBL of Finke et al, and calculate self-consistently the resulting spectrum by integrating over redshift. Of course, this can be done assuming other types of neutrino input sources too, which may have a different redshift dependence.

References

Bottcher, M. & Schlickeiser, R. A&A, 325, 866
Finke, J. D., Razzaque, S., & Dermer, C. D. 2010, ApJ , 712, 238
Hascoet, R. et al. 2012, MNRAS, 421, 525
Lacki, C. B., Horiuch, S. & Beacom, F. J. 2014, ApJ, 786, 40
Péer, A. & Waxman, E. 2005, ApJ, 628, 857
Pilla, R. P. & Loeb, A. 1998, ApJ, 494, L167
Pilla, R. P., & Shaham, J. 1997, ApJ, 486, 903
Ramaty, R. & Mészáros, P. 1981, ApJ, 250, 384
Senno, N. et al. 2015, ApJ, 806, 24